

An Effective Image Copy-Move Forgery Detection Using Entropy Information

Li Jiang

School of Electrical and Information Engineering
Zhengzhou University
Zhengzhou, China
ieljiang@zzu.edu.cn

Zhaowei Lu*

School of Electrical and Information Engineering
Zhengzhou University
Zhengzhou, China
luzhaoweizzu@163.com
*Corresponding author

Abstract—Image forensics has become increasingly crucial in our daily lives. Among various types of forgeries, copy-move forgery detection has received considerable attention within the academic community. Keypoint-based algorithms, particularly those based on Scale Invariant Feature Transform, have achieved promising outcomes. However, most of keypoint detection algorithms failed to generate sufficient matches when tampered patches were occurred in smooth areas, leading to insufficient matches. Therefore, this paper introduces entropy images to determine the coordinates and scales of keypoints based on Scale Invariant Feature Transform detector, which make the pre-processing more suitable for solving the above problems. Furthermore, an overlapped entropy level clustering algorithm is developed to mitigate the increased matching complexity caused by the non-ideal distribution of gray values in keypoints. Experimental results demonstrate that our algorithm achieves a good balance between performance and time efficiency.

Index Terms—Image forensics, copy-move forgery detection, Scale Invariant Feature Transform, entropy level clustering

I. INTRODUCTION

With the advancement of multimedia technology, the quality of digital image forgeries has improved significantly. Simultaneously, the cost associated with such forgeries has decreased. Consequently, it has become increasingly challenging for people to trust the authenticity of images, unlike several decades ago. Among the various manipulations, copy-move operation is particularly challenging due to its inherent similarity. Conventionally, Copy-Move Forgery Detection (CMFD) can be mainly divided into keypoint-based algorithms [1]–[8] and block-based algorithms [9], [10]. Currently, with the rise of deep learning developed, deep-based algorithms [11]–[15] have gradually been applied in this field. The main differences between conventional algorithms and deep-based algorithms are as follows:

- Deep-based algorithms outperform conventional on low-resolution images, but they usually rely on downsampling to detect high-resolution images; Conventional algorithms can detect all image sizes, but take longer with high-resolution images and rely on hand-crafted features for computer vision tasks.
- Deep-based algorithms still lack interpretability, while conventional algorithms are known for their good interpretability.

- Deep-based algorithms can be used to distinguish between source and target regions, while conventional algorithms struggle with this task.

Although deep-based algorithms have achieved great results, downsampling strategies for processing high-resolution images may lose important information, resulting in detection failure. Therefore, it is still necessary to continue to develop the conventional CMFD algorithm. This paper conducted research on the popular keypoint-based algorithms in CMFD. In existing works, detecting keypoints in gray images are the most commonly applied methods [1], [3]–[6]. However, gray images primarily represent brightness, making conventional keypoint detection algorithms less effective in regions with low texture. To address these issues, this paper proposed an effective CMFD algorithm, which mainly includes:

- This paper introduces entropy images to determine the coordinates and scales of keypoints based on Scale Invariant Feature Transform (SIFT) detector [16]. Since SIFT features represent the gradient information of the grayscale, the keypoints redefine orientation and extraction feature in gray image, which make matching stage more accuracy.
- This paper develops an overlapped entropy level clustering algorithm, which greatly reduces computation complexity caused by non-ideal grayscale distribution of keypoints.

The remainder of this paper is organized as follows. Related work is reported in section II. Our proposed method is introduced in section III. Experimental results are given in section IV, and section V draws the conclusion.

II. RELATED TECHNIQUE

A. Review Of The SIFT

Classical SIFT consists of the following four steps [16]:

- determining candidate points in Difference of Gaussian (DoG) space.
- selecting keypoints using contrast threshold T_{con} .
- calculating the dominant orientation.
- generating the feature descriptor.

Suppose there is a gray image I_{gray} , the candidate points are extracted by searching local extrema within $3 \times 3 \times 3$ DoG space regions. The DoG image D at scale σ is given by:

$$D(x, y, \sigma) = L(x, y, k\sigma) - L(x, y, \sigma) \quad (1)$$

Here, k is a predefined constant, (x, y) represents coordinates, and L means the gaussian image of I_{gray} . Mathematically, L can be defined as:

$$L(x, y, \sigma) = I_{gray}(x, y) \otimes G(x, y, \sigma) \quad (2)$$

Here, G and \otimes represent the Gaussian kernel and convolution operation, respectively. By applying Equation (1), multiple DOG spaces are generated at various scales.

Subsequently, the contrast values $|D(\mathbf{x})|$ in the candidate points are calculated:

$$|D(\mathbf{x})| = |D + \frac{1}{2}(\frac{\partial D}{\partial \mathbf{x}})^T \mathbf{x}| \quad (3)$$

Here, \mathbf{x} represents the coordinates of the candidate points. If the contrast value of candidate point is greater than the contrast threshold T_{con} , the candidate point will be selected as a keypoint.

Finally, the keypoints \mathbf{KP} and features \mathbf{F} will be represented as:

$$\mathbf{KP} = \{\mathbf{x}, \mathbf{y}, \sigma, \theta\} \quad (4)$$

$$\mathbf{F} = \{\mathbf{f}_1, \mathbf{f}_2, \dots, \mathbf{f}_{128}\} \quad (5)$$

Here, \mathbf{F} represents 128-dimensional features, and θ represents dominant orientation:

$$\theta = \arctan\left(\frac{L(x, y + 1) - L(x, y - 1)}{L(x + 1, y) - L(x - 1, y)}\right) \quad (6)$$

B. Detect Smooth Or Small Tampering

In recent years, the most important challenge facing CMFD is how to accurately detect tampering in small or smooth areas. In order to solve the above two problems, the SIFT algorithm has two strategies. The first strategy is reducing the contrast threshold. Compared with the results of the classical SIFT algorithm shown in Fig. 1 (a), the strategy of reducing the contrast threshold shown in Fig. 1 (b) can significantly increase the number of keypoints in the smooth region. The second strategy is image upsampling. This strategy aims to increase the number of keypoints per unit region of the original image. Through a reasonable number of upsampling, we can obtain sufficient keypoints for tampering localization. However, these two strategies are often only used for gray images.

Compared to gray images, entropy images can more effectively quantify the contrast of local region textures, resulting in a denser distribution of keypoints obtained using entropy images. As shown in Fig. 2 (a), three different types of images are selected from the GRIP dataset [9]. Then, the gradient information of gray images and entropy images are extracted to represent contrast information. The more high-contrast information, the more keypoints are generated. To enhance the visual experience for readers, the gray image contrast Fig. 2 (b) and entropy image contrast Fig.2 (c) results



Fig. 1. Keypoint detection by (a) classical contrast threshold; (b) reducing contrast threshold.

are normalized to the range $[0, 1]$ and displayed using pseudo-color images. Obviously, Entropy images have better contrast information.

Besides, there is an overlooked issue at this stage, that is, how do we determine the distribution of keypoints to meet our needs? Some pioneers have done some research. For example, in existing work [1], the patches with the minimum variance were extracted to ensure that each patch generates 4 keypoints on GRIP [9]. This is necessary because RANSAC estimation [17] requires a minimum of 4 correct matches; As the keypoint-based algorithms just published, Wang et al. [6] normalized the long edge of the low-resolution image to 3000 pixels to obtain a great keypoint distribution.

For the CMFD feature matching task, once the size of the descriptor is larger than the tampering size, there is insufficient evidence to prove that the matching is caused by the similarity of the tampered area. Based on this assumption, this paper believes that the distribution of keypoints should satisfy the requirement to generate 4 keypoints within the feature block size. Since the commonly used block sizes for extracting invariant moment features range from 12×12 to 32×32 , this paper adopts 16×16 . Fig. 2 (d) and (e) show the number of keypoints in the 16×16 region of the gray image and entropy image, respectively. Obviously, the entropy image suits this task better since it fulfills the paper's assumptions in more regions. For detailed quantization results, please refer to Fig. 6 (a).

III. PROPOSED METHOD

As shown in Fig. 3, the framework of the proposed algorithm consists of three stage. Firstly, the input image goes through the gray box to generate an entropy image, keypoints and corresponding features in the pre-processing stage. Then, keypoints are matched through hierarchical clustering represented by the yellow box in the matching stage. Finally, the method described in literature [1] represented by the blue box will be used in the post-processing stage. This post-processing was designed by fully exploiting the dominant orientation and scale information of each matched keypoint. Experimental results demonstrate that our algorithm achieves a good balance between performance and time efficiency.

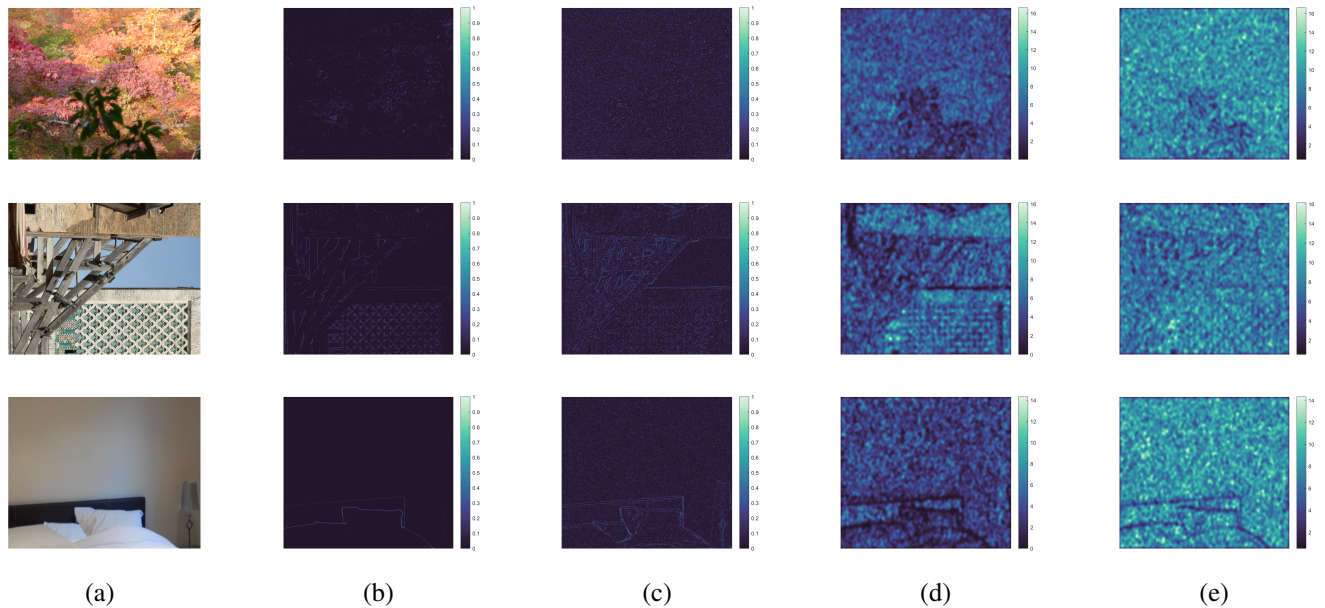


Fig. 2. Pre-processing results of different types of images. (a) RGB image; (b) the gradient information of gray image; (c) the gradient information of entropy image; (d) the number of keypoints within 16×16 in gray images; (e) the number of keypoints within 16×16 in entropy images.

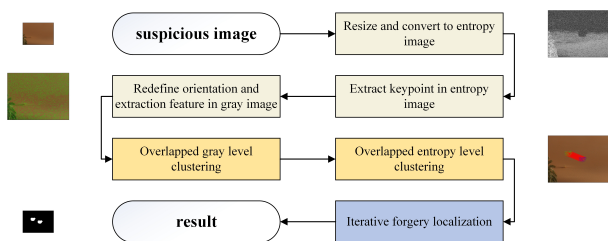


Fig. 3. Framework of the proposed algorithm.

A. Pre-processing

Assuming the input gray image is denoted as I_o . Then, the resized gray image I_{gray} is defined as:

$$I_{gray} = \text{imresize}(I_o, s) \quad (7)$$

Here, $\text{imresize}(\cdot)$ and s denotes image resize function and resize factor, respectively. Bicubic linear interpolation is used in this paper. For instance, if I_o with dimensions 1024×728 and resize it with $s = 2$, I_{gray} will have dimensions of 2048×1456 .

Then, the entropy image $I_E(x, y)$ at position (x, y) can be expressed as:

$$I_E(x, y) = \sum_{i=0}^{255} p_i(x, y) \cdot \log_2[p_i(x, y)] \quad (8)$$

Here, $p_i(x, y)$ represents the probability of the grayscale value being i in a square region with radius R_E around (x, y) . I_E can be obtained by performing the same steps on I_{gray} .

Next, the SIFT detector is applied to extract keypoints \mathbf{KP}_E from I_E . \mathbf{KP}_E can be defined as follows:

$$\mathbf{KP}_E = \{\mathbf{x}_E, \mathbf{y}_E, \sigma_E, \theta_E\} \quad (9)$$

Here, $(\mathbf{x}_E, \mathbf{y}_E)$ represent the image plane coordinates, σ_E denote scale information. The dominant orientation θ_E of keypoints \mathbf{KP}_E are then redefined on the gray image through Equation (6), and features \mathbf{F} are extracted from I_{gray} . Finally, \mathbf{KP} can be defined as follows:

$$\mathbf{KP} = \{\mathbf{x}_E, \mathbf{y}_E, \sigma_E, \theta_{gray}\} \quad (10)$$

B. Hierarchical Keypoint Clustering Matching

Gray value is widely used in keypoint clustering algorithms as it effectively represents the fundamental information of an image. The major advantage of these methods is conducted in a much more efficient way without deleting original correct matches. In this paper, an overlapped gray level clustering method [1] is introduced.

Although overlapped gray level clustering can be conducted in an effective way, its efficiency may decrease when the gray values of keypoints are concentrated within a specific range. Fig. 4 (a) shows the gray distribution of the keypoints obtained from a certain suspicious image. The gray values of keypoints are concentrated in the range of $[150, 200]$. Our statistical analysis indicates that around 70% of keypoints fall within this range. This will greatly reduce the efficiency of clustering matching.

To overcome this challenge, the overlapped entropy level clustering is developed. From Fig. 4 (b), it is evident that the entropy distribution exhibits a favorable pattern even in cases where the gray distribution is not ideal. Therefore, it is possible to partition the gray values and entropy values of the two-dimensional plane in a reasonable way.

After that, this paper will explain the hierarchical clustering algorithm. Formally, the group of overlapped gray level

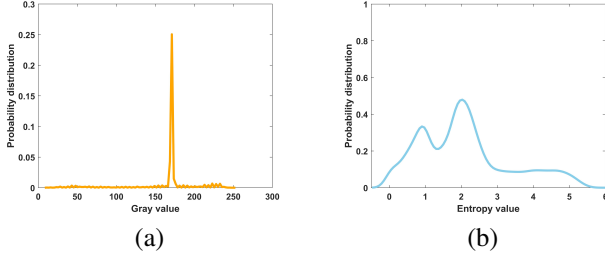


Fig. 4. An example of hierarchical feature point clustering. (a) the gray value distribution of the keypoints; (b) the entropy value distribution of the keypoints.

clustering C^u can be expressed as:

$$\begin{cases} C^u = \{kp_i | I_{gray}(kp_i) \in [a_l^u, a_h^u], kp_i \in \mathbf{KP}\} \\ a_l^u = (u - 1) \cdot (step_1 - step_2) \\ a_h^u = \min(a_l^u + step_1, 255) \end{cases} \quad (11)$$

Here, $step_1$ represents the interval size, $step_2$ represents the overlapped size ($step_1 > step_2$). The number of gray level groups is denoted as N_u , and can be computed using the following equation:

$$N_u = \left\lceil \frac{255 - step_1}{step_1 - step_2} \right\rceil + 1 \quad (12)$$

The overlapped entropy level clustering algorithm can be expressed as follows:

$$\begin{cases} C^{u,v} = \{kp_i | I_E(kp_i) \in [a_l^{u,v}, a_h^{u,v}], kp_i \in C^u\} \\ a_l^{u,v} = \max(0, (v - 1) \cdot step_3 - step_4) \\ a_h^{u,v} = \min(7, v \cdot step_3 + step_4) \end{cases} \quad (13)$$

Due to the fact that entropy values are controlled by R_E , it is evident that all entropy values are distributed within the range of $[0, 7]$ (In this paper, $R_E = 3$, so the theoretical maximum value of entropy is $-\log_2(P) = -\log_2(1/(2 \cdot R_E + 1)^2) \approx 5.61$). The number of entropy level groups for group C^u is denoted as $N_{u,v}$. Obviously, $N_{u,v}$ can be computed using the following equation:

$$N_{u,v} = \left\lceil \frac{7 - step_4}{step_3} \right\rceil \quad (14)$$

Once hierarchical keypoint clustering is implemented, the next step involves matching $C^{u,v}$, while ensuring that the matching process meets the following condition:

$$d_i < T \cdot d_{i+1}, i = 2, \dots, n_{u,v} \quad (15)$$

Here, $n_{u,v}$ represents the number of keypoints within $C^{u,v}$'s group, d represents the ascending distance between a certain feature and all features within $C^{u,v}$. Obviously, d_1 represents the distance between the feature and itself, so $d_1 = 0$. For the matching stage, this paper maintains Amerini's [7] setting ($T = 0.5$). For the post-processing stage, we follow the iterative forgery localization algorithm used in reference [1].

IV. EXPERIMENTS

In this section, our proposed method is evaluated through a series of simulation experiments. All the experiments are done using MATLAB R2018a under Microsoft Windows. The PC used for testing has 2.30 GHz CPU and 16 GB RAM. Our code is available at <https://github.com/LUZW1998/CMFDUEI>.

A. Datasets

This paper validates the proposed algorithm using two public datasets, with details as follows:

- GRIP: This dataset [9] contains 80 tampered images and 80 original images, all of which are in the size of 1024×768 pixels.
- CMH: This dataset [2] consists of 108 tampered images with resolutions ranging from 845×634 to 3888×2592 pixels.

For details on the tampering included in each dataset, please see Table I.

TABLE I
TAMPERING TYPES OF DATASET

dataset	translation	Rotation	Scaling
GRIP	✓		
CMH	✓	✓	✓

B. Evaluation Metrics

Generally, the evaluation of CMFD techniques can be performed at two levels: image level and pixel level. At the image level, the objective is to accurately determine whether an image is tampered with or original. At the pixel level, a more stricter criterion is applied, emphasizing the localization of tampered regions within the image. Usually, datasets commonly employ three evaluation metrics, which are defined as follows:

$$TPR = \frac{TP}{TP + FN} \quad (16)$$

$$FPR = \frac{FP}{TN + FP} \quad (17)$$

$$F = \frac{2TP}{2TP + FP + FN} \quad (18)$$

In the equation mentioned above, TP represents the number of correctly detected tampered images or pixels, TN represents the number of correctly detected original images or pixels, FN represents the number of incorrectly detected tampered images or pixels, and FP represents the number of incorrectly detected original images or pixels. To provide more detailed test results, TPR and FPR are used to represent image-level TPR and FPR metrics, while $F-i$ and $F-p$ represent image-level and pixel-level F metrics, respectively.

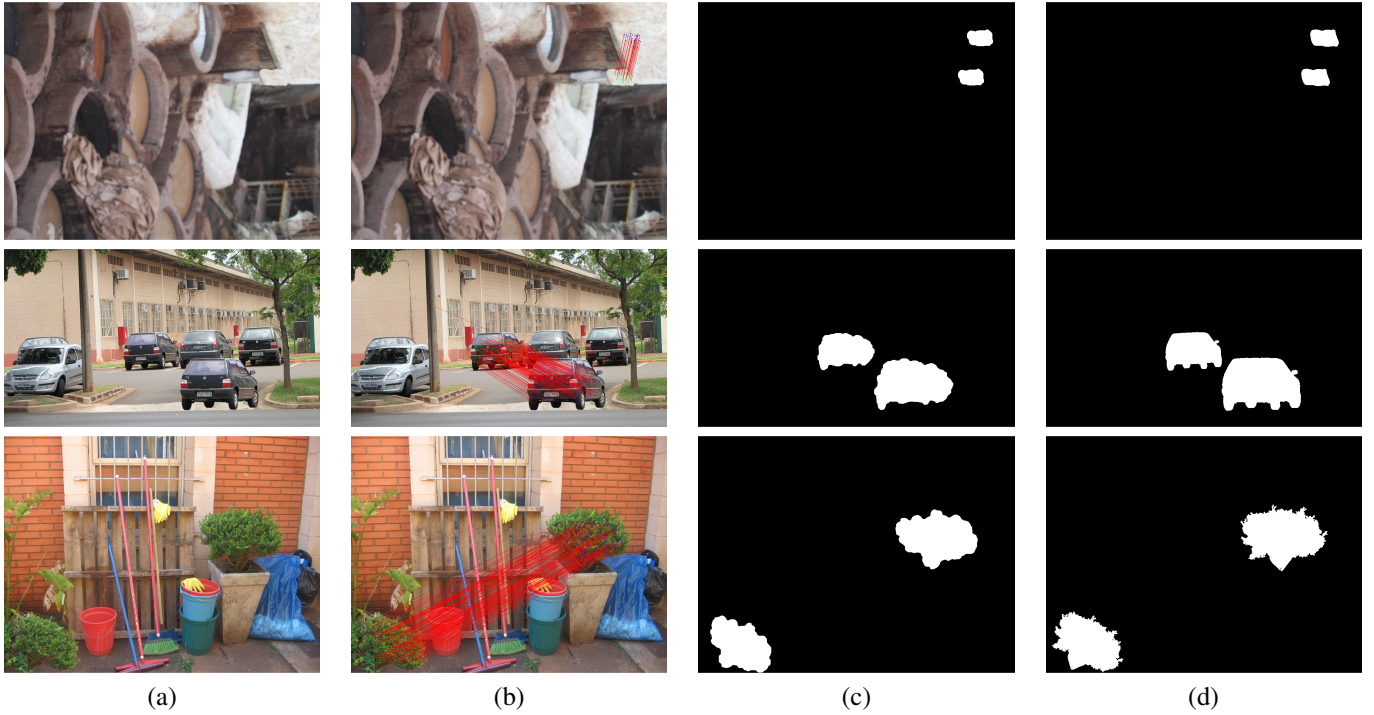


Fig. 5. Some experimental results. (a) forgery images; (b) matching; (c) binary result; (d) ground-true.

C. Analysis Of Parameters

In this subsection, this paper mainly analyzes the pre-processing resize factor s and entropy radius R_E , as well as the matching process parameters $step_3$ and $step_4$.

As shown in Fig. 6 (a), this paper calculates the ratio of meeting the assumption (II-B) under different s . As resize factor s increases, more pixel patches have 4 keypoints. Obviously, when the resize factor s is the equal, there is considerable evidence that the entropy image is more suitable for CMFD. In this paper, we adopt $s = 2$.

As shown in Fig. 6 (b), this paper calculates the ratio of meeting the assumption under different R_E . Furthermore, the ratio of meeting the assumption in gray images is only 69.99%. Clearly, entropy images yields better results compared to gray images when R_E is within the range [2, 6], and the highest performance occurs at $R_E = 3$. Therefore, this paper adopts $R_E = 3$.

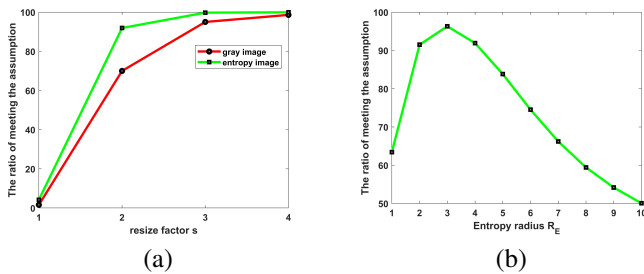


Fig. 6. The analysis of pre-processing. (a) the ratio of meeting the assumption under different resize factor s ; (b) The ratio of meeting the assumption under different entropy radius R_E .

Considering that the robustness of entropy values may diminish when facing geometric transformation, the fourth group of images from the CMH dataset are used for brute force matching and analyze the distribution of entropy values for correct matches. To quantify $step_3$, this paper calculates the entropy difference between correct matches. Then, the cumulative probability is obtained, as shown in Fig. 7 (a). This paper believes that the entropy difference for correct matches lies in the range of [0, 1] (The cumulative probability reaches 99.77% at $step_3 = 1$). Therefore, this paper chooses $step_3 = 1$.

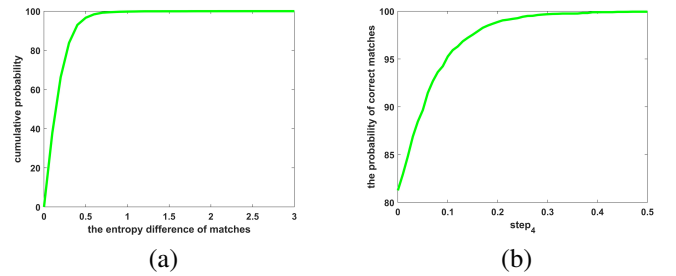


Fig. 7. The analysis of overlapped entropy level clustering. (a) the cumulative probability of the entropy difference of matches; (b) the number of correct matches relative to brute force matching under different $step_4$.

As shown in Fig. 7 (b), statistical analysis is conducted with a step size of 0.01 over the range of [0, 0.5]. Based on observation, the correct matching reached 81.26% when $step_4 = 0$. As $step_4$ increases, the rate of correct matches relative to brute force matching continues to rise in the overlapped entropy clustering. Considering that a larger overlapped interval leads

to higher matching complexity, this paper adopts $step_4 = 0$ (If readers want to accelerate using ANN, this paper recommends $step_4 = 0.2$, which achieves an accuracy rate of 99.04%).

D. Performance Comparison On Different Datasets

In this work, a combined dataset named CMH+GRIPori is adopted, consisting of all the 108 forgeries from CMH, and the 80 original images from GRIP dataset. Some results of the testing are shown in Fig. 5.

Table II lists the performance comparison of different algorithms on CMH+GRIPori dataset, including keypoint-based [1]–[3], [6], block-based [9] and the proposed method. Obviously, our proposed method achieves the best results in comparison with the current best classical algorithms.

TABLE II
PERFORMANCE COMPARISON OF DIFFERENT ALGORITHMS ON THE
CMH+GRIPORI DATASET

methods	TPR	FPR	F-i	F-p	time
[1]	96.3	0	98.11	90.61	11.2s
[2]	95.37	38.75	85.12	64.09	18.1s
[3]	99.07	0	99.53	91.72	43.3s
[6]	99.07	11.25	95.54	91.09	22.2s
[9]	92.59	8.75	93.02	88.10	13.1s
proposed	99.07	0	99.53	92.47	19.9s

Table III lists the performance comparison of different algorithms on GRIP. It can be observed that our proposed method achieves great results on this dataset as well. However, our proposed method has shortcomings in terms of time complexity, but this is not due to the design of the matching stage. In our statistics, our proposed method obtains approximately 1.5 times the number of keypoints compared to the generated gray images. Typically, the time complexity is directly proportional to the square of the number of keypoints. Based on this estimation, our matching efficiency is approximately 29% faster than the state-of-the-art method mentioned in reference [3] when tested on the GRIP dataset.

TABLE III
PERFORMANCE COMPARISON OF DIFFERENT ALGORITHMS ON THE GRIP
DATASET

methods	TPR	FPR	F-i	F-p	time
[1]	100	0	100	94.66	13.9s
[2]	100	38.75	83.77	66.62	11.7s
[3]	100	0	100	98.57	12.9s
[6]	100	11.25	94.67	85.71	21.5s
[9]	98.75	8.75	95.18	92.99	14.8s
proposed	100	0	100	95.47	20.6s

V. CONCLUSION

In this paper, a novel framework is proposed using entropy information, which can be used for CMFD. Firstly, entropy images are introduced to determine the coordinates and scales space of keypoints. Considering SIFT features represent the gradient information of the grayscale, the keypoints redefine orientation and extraction feature in gray image, which makes our matching process more accuracy. Then, an entropy level

clustering is developed to avoid increased matching complexity caused by non-ideal distribution of grayscale in keypoints. Experimental results demonstrate that our algorithm achieves a good balance between performance and time efficiency.

REFERENCES

- [1] Yuanman Li and Jiantao Zhou, "Fast and effective image copy-move forgery detection via hierarchical feature point matching," *IEEE Transactions on Information Forensics and Security*, vol. 14, no. 5, pp. 1307–1322, 2018.
- [2] Ewerton Silva, Tiago Carvalho, Anselmo Ferreira, and Anderson Rocha, "Going deeper into copy-move forgery detection: Exploring image telltales via multi-scale analysis and voting processes," *Journal of Visual Communication and Image Representation*, vol. 29, pp. 16–32, 2015.
- [3] Pan-pan Niu, C Wang, W Chen, Hongying Yang, and Xiangyang Wang, "Fast and effective keypoint-based image copy-move forgery detection using complex-valued moment invariants," *Journal of Visual Communication and Image Representation*, vol. 77, pp. 103068, 2021.
- [4] Patrick Niyishaka and Chakravarthy Bhagvati, "Copy-move forgery detection using image blobs and brisk feature," *Multimedia Tools and Applications*, vol. 79, no. 35-36, pp. 26045–26059, 2020.
- [5] Qiyue Lyu, Junwei Luo, Ke Liu, Xiaolin Yin, Jiarui Liu, and Wei Lu, "Copy move forgery detection based on double matching," *Journal of Visual Communication and Image Representation*, vol. 76, pp. 103057, 2021.
- [6] Chao Wang, Zhiqiu Huang, Shuren Qi, Yaoshen Yu, Guohua Shen, and Yushu Zhang, "Shrinking the semantic gap: spatial pooling of local moment invariants for copy-move forgery detection," *IEEE Transactions on Information Forensics and Security*, vol. 18, pp. 1064–1079, 2023.
- [7] Irene Amerini, Lamberto Ballan, Roberto Caldelli, Alberto Del Bimbo, and Giuseppe Serra, "A sift-based forensic method for copy-move attack detection and transformation recovery," *IEEE transactions on information forensics and security*, vol. 6, no. 3, pp. 1099–1110, 2011.
- [8] Amarpreet Singh and Sanjogdeep Singh, "Gray level co-occurrence matrix with binary robust invariant scalable keypoints for detecting copy move forgeries," *Journal of Image and Graphics*, vol. 11, no. 1, 2023.
- [9] Davide Cozzolino, Giovanni Poggi, and Luisa Verdoliva, "Efficient dense-field copy-move forgery detection," *IEEE Transactions on Information Forensics and Security*, vol. 10, no. 11, pp. 2284–2297, 2015.
- [10] Seung-Jin Ryu, Matthias Kirchner, Min-Jeong Lee, and Heung-Kyu Lee, "Rotation invariant localization of duplicated image regions based on zernike moments," *IEEE Transactions on Information Forensics and Security*, vol. 8, no. 8, pp. 1355–1370, 2013.
- [11] Yingjie He, Yuanman Li, Changsheng Chen, and Xia Li, "Image copy-move forgery detection via deep cross-scale patchmatch," in *2023 IEEE International Conference on Multimedia and Expo (ICME)*. IEEE, 2023, pp. 2327–2332.
- [12] Yue Wu, Wael Abd-Almageed, and Prem Natarajan, "Busternet: Detecting copy-move image forgery with source/target localization," in *Proceedings of the European conference on computer vision (ECCV)*, 2018, pp. 168–184.
- [13] Beijing Chen, Weijin Tan, Gouenou Coatrieux, Yuhui Zheng, and Yun-Qing Shi, "A serial image copy-move forgery localization scheme with source/target distinguishment," *IEEE Transactions on Multimedia*, vol. 23, pp. 3506–3517, 2020.
- [14] Ashrafal Islam, Chengjiang Long, Arslan Basharat, and Anthony Hoogs, "Doa-gan: Dual-order attentive generative adversarial network for image copy-move forgery detection and localization," in *Proceedings of the IEEE/CVF conference on computer vision and pattern recognition*, 2020, pp. 4676–4685.
- [15] Jun-Liu Zhong, Ji-Xiang Yang, Yan-Fen Gan, Lian Huang, and Hua Zeng, "Coarse-to-fine spatial-channel-boundary attention network for image copy-move forgery detection," *Soft Computing*, vol. 26, no. 21, pp. 11461–11478, 2022.
- [16] David G Lowe, "Distinctive image features from scale-invariant keypoints," *International journal of computer vision*, vol. 60, pp. 91–110, 2004.
- [17] Martin A Fischler and Robert C Bolles, "Random sample consensus: a paradigm for model fitting with applications to image analysis and automated cartography," *Communications of the ACM*, vol. 24, no. 6, pp. 381–395, 1981.